Structural and magnetic characterization of superparamagnetic iron platinum nanoparticle contrast agents for magnetic resonance imaging

Robert M. Taylor[a]
University of New Mexico, Department of Biochemistry and Molecular Biology, MSC08 4670, 1 University of New Mexico, Albuquerque, New Mexico 87131 and New Mexico Cancer Nanoscience and Microsystems Training Center, Albuquerque, New Mexico 87106

Dale L. Huber
Sandia National Laboratories, Center for Integrated Nanotechnologies, P.O. Box 5800 MS 1304, Albuquerque, New Mexico 87111-1304

Todd C. Monson
Sandia National Laboratories, Nanomaterials Sciences Department, Albuquerque, New Mexico 87185-1415

Victor Esch
nanoMR, Inc., 2305 Renard Place SE, Suite 110, Albuquerque, New Mexico 87106

Laurel O. Sillerud
University of New Mexico, Department of Biochemistry and Molecular Biology, MSC08 4670, 1 University of New Mexico, Albuquerque, New Mexico 87131 and UNM Cancer Center, 1201 Camino de Salud NE, Albuquerque, New Mexico 87106

The authors report the synthesis, from simple salts, and the physical characterization of superparamagnetic iron platinum nanoparticles (SIPPs) suitable for use as contrast agents in magnetic resonance imaging. The properties of these particles were determined by means of transmission electron microscopy (TEM), thermogravimetric analysis, inductively coupled plasma-optical emission spectroscopy (ICP-OES), superconducting quantum interference device (SQUID) magnetometry, and nuclear magnetic resonance relaxivity at 4.7 T. TEM showed that the diameters of the particles ranged from 9.3 to 10 nm, depending on the mole ratio of iron to platinum precursors, and on the concentration of octadecylamine (ODA) used in their preparation. The iron to platinum stoichiometry determined by ICP-OES varied from 1.4:1 to 3.7:1 and was similarly dependent on the initial mole ratios of iron and platinum salts, as well as on the concentration of ODA in the reaction. SQUID magnetometry showed that the SIPPs were superparamagnetic and had magnetic moments that increased with increasing iron content from 62 to 72 A·m^2/kg Fe. The measured relaxivities of the SIPPs at 4.7 T were higher than commercially available superparamagnetic iron oxide nanoparticles, suggesting that these particles may be superior contrast agents in T$_2$-weighted magnetic resonance imaging. © 2012 American Vacuum Society. [http://dx.doi.org/10.1116/1.3692250]

I. INTRODUCTION

Ferromagnetic face-centered tetragonal iron platinum (FePt) nanoparticles have frequently been synthesized, for use in magnetic storage devices, by annealing superparamagnetic iron platinum particles (SIPPs) at elevated temperatures.[1–6] The precursor SIPPs have also found a niche as contrast agents in magnetic resonance imaging (MRI).[7–9] Magnetic nanoparticles that cause larger perturbations in the relaxation times of water molecules in close proximity to the particles typically have higher magnetic moments and SIPPs have been reported to have extremely high volume magnetizations between 6×10^5 and 1×10^6 A/m.[9–12] These high volume magnetizations suggest that SIPP syntheses could be optimized to be superior MRI contrast agents. Once developed, biocompatible SIPP contrast agents will also need to go through animal toxicity studies, as this information is not currently available.

Iron pentacarbonyl, Fe(CO)$_5$, is a hazardous reagent that is frequently used in the synthesis of magnetic nanoparticles.[3,5,13] We have previously described, along with others, a synthesis method to produce SIPPs that are ~ 9 nm in diameter using simple iron and platinum salts and the ligand octadecylamine (ODA) as the stabilizing ligand.[9,10] This synthesis tends to be a safer and environmentally friendlier method, as it uses less toxic reagents and ODA acts as both the solvent and the ligand; thus reducing the number of reagents needed. Here, we describe the synthesis of SIPPs using different concentrations of the salt precursors and ODA and show that the sizes and magnetic moments of these particles can be tailored by controlling both the initial mole ratios of the precursor metal salts and the concentration of ODA in the reaction mixture. The SIPPs described here were also refluxed for a shorter duration of time (30 min) and heated to a higher temperature (340 °C) than previously reported.[9] Furthermore, we describe the physical and magnetic characterization of the nanoparticles resulting from these various syntheses and show that SIPPs are superior

[a]Electronic mail: rmtaylor@salud.unm.edu

T_2-weighted contrast agents for MRI, when compared to superparamagnetic iron oxide nanoparticles (SPIONs).

II. EXPERIMENT

A. Materials

Iron nitrate nonahydrate ($Fe(NO_3)_3 \cdot 9H_2O$), platinum (II) acetylacetonate ($Pt(Acac)_2$), and 1-octadecylamine (ODA) were purchased from Fisher Scientific (Pittsburgh, PA). Nonylphenoxy propenyl polyethylate alcohol (RN-10) was a generous gift from Dai-Ichi Kogyo Seiyaku (Kyoto, Japan). The temperature controller (model 210-J) was purchased from J-KEM Scientific, Inc. (St. Louis, MO). Heating mantles were purchased from Glas-Col, LLC (Terre Haute, IN) and glassware was purchased from Quark Glass (Vineland, NJ). Superparamagnetic iron oxide nanoparticles (SPIONs) were purchased from Miltenyi Biotec as their μMAC product. All other chemicals and supplies were purchased from common manufacturers.

B. SIPP synthesis

Nanoparticles were synthesized using a modification of a procedure due to Taylor *et al.*[9] and Zhao *et al.*[10] For SIPP#1, 1.0 mmol $Fe(NO_3)_3 \cdot 9 H_2O$ and 1.0 mmol $Pt(Acac)_2$ were added to 12.5 mmol ODA in a 25 mL 3 neck round bottom flask fitted with a reflux condenser. After the apparatus was assembled, the reaction was heated to $340\,^{\circ}C$ at a rate of $200\,^{\circ}C/h$. Refluxing at $340\,^{\circ}C$ was continued for 30 min at which point the reaction was removed from the heat and allowed to cool to room temperature. The resulting black particles were collected in hexane and subjected to repeated ethanol washes with centrifugation. SIPP#2 and SIPP#3 were prepared in the same manner as SIPP#1 except 1.0 mmol $Fe(NO_3)_3 \cdot 9 H_2O$ and 1.0 mmol $Pt(Acac)_2$ were added to 25.0 mmol ODA for SIPP#2, while 2.0 mmol $Fe(NO_3)_3 \cdot 9 H_2O$ and 1.0 mmol $Pt(Acac)_2$ were added to 12.5 mmol ODA for SIPP#3. The SIPPs were resuspended in hexane and stored at room temperature. A typical synthesis as described above produced $\sim$20 mg of SIPPs.

C. Physical characterization of SIPPs

Transmission electron microscopy (TEM) was used to determine the size and polydispersity of the particle populations. A drop of the hexane suspension of the SIPPs was applied to carbon-coated grids. After the solvent evaporated, the samples were imaged on a Hitachi 7500 transmission electron microscope with an acceleration voltage of 80 kV. Particle diameters were calculated using IMAGEJ software.[14] At least 1000 particles were counted and the mean Feret diameters and standard deviations were calculated. The compositions of the SIPPs were investigated with thermogravimetric analysis (TGA). Aliquots of SIPPs were evaporated in TGA sample cups (Robocasting Enterprises LLC, Albuquerque, NM) and allowed to evaporate. Weight loss profiles were measured with a SDT Q600 TGA/DSC (TA Instruments, New Castle, DE) under nitrogen flow. The ODA and FePt content were determined by measuring the mass change

while the temperature was raised from room temperature to $1000\,^{\circ}C$ at a $20\,^{\circ}C/min$ heating rate. Inductively coupled plasma-optical emission spectroscopy (ICP-OES) was used to measure the metal content and iron to platinum stoichiometry of each synthesis. Prior to analysis, gentle refluxing with nitric and hydrochloric acids digested aliquots of SIPPs. After cooling, the samples were made up to volume, mixed and centrifuged. Samples were then analyzed using a PerkinElmer Optima 5300DV ICP-OES using the recommended wavelengths for each of the analytes. Analysis was performed in an axial mode to improve detection limits. A blank and set of calibration standards were used to establish a three-point calibration curve. Calibration verification samples (ICBV and ICV) were analyzed prior to analyzing the samples. Analyte peaks were examined and peak locations and background points were adjusted for optimum recoveries.

D. Magnetic characterization of SIPPs

Superconducting quantum interference device (SQUID) magnetometry was used to measure the blocking temperatures and saturation magnetizations of the SIPPs. Aliquots (100 μL) of the hexane suspension of SIPPs were placed in 5 mm, economy 8-in. nuclear magnetic resonance (NMR) tubes (Wilmad LabGlass, Vinelanad NJ, USA) and allowed to evaporate overnight. Magnetic measurements were made on a Quantum Design MPMS-7 SQUID magnetometer. Temperature sweeps between 0 and 400 K were performed by zero-field cooling the sample and then measuring the magnetic moment as a function of temperature under the influence of a weak magnetic field (1 mT) during warming and subsequent cooling. This procedure yields both a zero-field-cooled (ZFC) and field-cooled (FC) curve, respectively. Values of the blocking temperature (T_B) were recorded by determining the peak location in each ZFC curve. Saturation magnetizations were measured at human body temperature (310 K) by varying the applied field from -5 to 5 T. Mass magnetizations were calculated with the known iron concentrations determined with ICP-OES. The iron to platinum ratio, determined with ICP-OES, was used to calculate the density of an fcc unit cell representing the naked SIPPs without ODA ligand. The weight percent of ODA on the particles, measured with TGA, was used with the density calculated for naked SIPPs to estimate the density of ODA coated SIPPs. Volume magnetizations were calculated using this calculated density for ODA coated SIPPs.

E. Magnetic resonance imaging and relaxivities

Increasing concentrations of SIPPs (0.02 to 0.3 mM iron) or SPIONs (0.1 to 0.62 mM iron) were added to 1% agarose in 2.0 mL self-standing micro-centrifuge tubes (Corning Inc., Corning, NY). Samples were imaged on a 4.7 T Bruker Biospin (Billerica, MA) MRI system with PARAVISION 4.0 software. Samples were imaged with a 512×256 matrix, a variable TE, and TR $= 10$ s. T_1 measurements were acquired by inversion-recovery with 15 interpulse delays. Spin- and gradient echo sequences were used to measure T_2, and T_2^*,

respectively. The MRI samples were then digested as above for ICP-OES and the iron concentration was determined. The relaxation rates, R_n ($= 1/T_n$), were calculated and plotted versus the ICP-OES-determined iron concentration of each sample. Linear regression was used to fit the data and the relaxivity (r_n) of each SIPP synthesis is given as the slope of the resulting line in units of Hz/mM Fe.

III. RESULTS AND DISCUSSION

SIPPs were synthesized using two different mole ratios of iron to platinum precursors, and with two different amounts of ODA. Table I outlines the general synthetic parameters used for each of the three SIPP syntheses that we report. We began by producing SIPPs using a 1:1 mol ratio of the metal salt precursors and 12.5 mmol of ODA (SIPP#1). Since iron provides the magnetism for these nanoparticles, we expected that increasing the amount of iron precursor would generate SIPPs with a greater Fe:Pt mole ratio and thus a higher magnetic moment. For this reason, we also synthesized SIPPs with a 2:1 mol ratio of iron to platinum, while keeping the amount of ODA at 12.5 mmol (SIPP#3). Additionally, we expected that the amount of ODA in the reaction mixture would affect the formation and final characteristics of the SIPPs. To explore this possibility, we synthesized SIPPs with a 1:1 molar ratio of iron to platinum and increased the amount of ODA to 25.0 mmol (SIPP#2). TEM images of particles from each SIPP synthesis are shown in Fig. 1. From the TEM images, it is seen that the nanoparticles are roughly spherical in shape. Using IMAGEJ software[8] to analyze the TEM images, we found that the SIPPs had average diameters that ranged from 9.3 ± 1.9 nm (SIPP#1) to 10 ± 3.4 nm (SIPP#3). This finding suggested that as the mole ratio of iron added to the reaction was increased, the size of the particles increased slightly. In addition, the size of the particles also increased as the concentration of ODA was increased in the reaction. To understand these trends, we used ICP-OES to determine the composition of the SIPPs and found that the iron to platinum stoichiometry increased with increasing iron precursor and ODA. Also of note, is that the polydispersity of the SIPPs increased with increasing size and Fe:Pt stoichiometry, as was evident by the increase in the standard deviation in the diameter describing the size distribution of the particles. Table II summarizes the physical and magnetic characteristics of the three SIPP syntheses, compared with commercially available SPIONs. It is clear that the amount of ODA plays an important role in the formation of the FePt alloy and the resultant iron to platinum stoichiometry. Zhao *et al.*[10] previously suggested that an excess of ODA was

TABLE I. Parameters used in the synthesis of SIPPs.

Sample	Molar ratio[a]	ODA (mmol)
SIPP#1	1	12.5
SIPP#2	1	25.0
SIPP#3	2	12.5

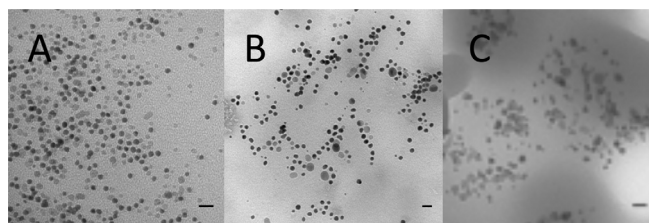[a]Molar ratio of $Fe(NO_3)_3 \cdot 9H_2O$:$Pt(Acac)_2$.

FIG. 1. Images of SIPPs acquired using transmission electron microscopy. Drops of SIPPs were applied to carbon-coated grids and the samples were imaged at an acceleration voltage of 80 kV. (a) SIPP#1, (b) SIPP#2, (c) SIPP#3. Scale bars = 20 nm.

needed in this particular synthetic method and that the initial decomposition of the iron and platinum salts led to three possible products; pure iron, iron oxides, or FePt nanoparticles. The excess ODA is thought to react with the iron oxides, forming an intermediate, $Fe(ODA)_3$ complex.[10] The catalytic activity of the FePt nanoparticles then provides a pathway available to the pure iron. It appears that by increasing the amount of ODA to 25.0 mmol, twice the amount previously used,[9,10] that more iron is deposited into the FePt alloy.

To further investigate the composition of the SIPPs, TGA was used to remove the organic layer on the particles and determine the weight percents of ODA and naked FePt. The TGA data for SIPP#1 is shown in Fig. 2. ODA has a boiling point around $347\,°C$ and; therefore, we suggest that the pronounced weight loss seen from ~ 300 to $400\,°C$ is due to the removal of ODA from the SIPP surface. It is plausible that some of this weight loss could also be due to iron oxides in the samples. The thermal decomposition of naked SPIONs has been reported to occur from 300 to $400\,°C$.[15] This overlap in the thermal decomposition temperatures of the ODA and iron oxides make it difficult to determine from the TGA data what percentage of the weight loss may or may not be due to iron oxide contaminants in the SIPPs. The TGA results suggest that the organic layer comprised approximately 20% of the particle mass, much less than previously reported with lower temperature preparations that used increased reaction times.[9,10] All of the syntheses showed similar decomposition curves and indicated that the SIPPS were between 18 and 22% ODA by mass.

We expected that increasing the concentration of iron per SIPP by increasing the mole ratio of iron to platinum in the reaction mixture would lead to a higher magnetic moment simply due to the larger amount of magnetic iron that would be present in each particle. We therefore determined the magnetic characteristics of the various SIPP syntheses using SQUID magnetometry. Figure 3 shows the mass magnetization as a function of the applied magnetic field for the three SIPP syntheses. In agreement with our expectations, both the mass magnetization and the volume magnetization increased with increasing iron content from SIPP#1 to SIPP#2. Once the iron to platinum ratio increased above 3.5, though, the volume magnetization began to decrease, while the mass magnetization continued to increase. We calculated the anisotropy of each SIPP synthesis based on the blocking

TABLE II. Physical and magnetic characteristics of SIPPs and SPIONs.

	Variable	Units	SIPP#1	SIPP#2	SIPP#3	SPIONs[a]
R	Fe:Pt ratio	—	1.44	2.35	3.67	—
D	Diameter of particle	nm	9.28	9.98	10.03	50[b]
σ	Standard deviation in diameter	nm	1.94	2.90	3.43	—
ρ	Density	g/cm^3	5.2	5.2	5.2	2.5[c]
M	Mass of iron per particle	pg	1.5×10^{-6}	2.2×10^{-6}	2.6×10^{-6}	1.6×10^{-5}
C_{Fe}	Fe concentration of solution	g/mL	1.2×10^{-3}	1.9×10^{-3}	2.8×10^{-2}	2.7×10^{-4} [c]
C_p	Particle concentration	Particles/mL	8×10^{14}	9×10^{14}	1×10^{16}	2×10^{14} [c]
T_b	Blocking temperature	Kelvin	170	210	195	155[c]
K	Effective anisotropy energy	J/m^3	1.4×10^5	1.4×10^5	1.3×10^5	1.2×10^5 [c,d]
μ_M	Mass magnetization	A m^2/kg Fe	61.7	69.2	71.8	82.0[c]
μ_V	Volume magnetization	A/m	7.4×10^5	7.4×10^5	6.8×10^5	2.0×10^5

[a]MACS® iron oxide particles from Miltenyi Biotec.
[b]Hydrodynamic diameter according to manufacturer.
[c]Taylor *et al.* (Ref. 9).
[d]Calculated using a magnetic core diameter of 10 nm.

temperature measured by SQUID magnetometry. The relationship between the anisotropy and the blocking temperature (K) is

$$K = \frac{25kT_B}{V}, \tag{1}$$

where k is Boltzmann's constant, T_B is the blocking temperature of the individual SIPP synthesis, and V is the volume of a single particle in units of cm^3. The constant 25 is calculated using a relaxation time of 1×10^{-9} s and a measurement time of 100 s. Table II shows that the anisotropy remained fairly constant for all of the SIPP syntheses. This did not support the idea that magnetic order increases with iron content. The effective anisotropy constants of the synthesized nanoparticles are in good agreement with magnetocrystalline anisotropy constants for SIPPs previously reported.[7,16] Further studies using high-resolution TEM and x-ray diffraction methods may be able to increase our understanding of any crystalline differences in the SIPPs synthesized.

Finally, to test whether the SIPPs could be beneficial as MRI contrast agents, we chose to examine SIPP#2, since it

had intermediate stoichiometry, size, and magnetic properties compared to the other SIPPs. Relaxivities were measured at 4.7 T for SIPP#2 and compared with relaxivities of ∼50 nm μMACs® (Miltenyi Biotec, Carlsbad, CA) SPIONs, also measured at 4.7 T. We first imaged the μMAC particles using TEM and measured their magnetization using SQUID magnetometry.[9] Figure 4 shows a representative TEM image of the μMACs SPIONs showing a mean magnetic core diameter of ∼20 nm, although the hydrodynamic diameters may be larger due to the fact that coatings on the particles are not visible using TEM. The manufacturer suggests that these dextran-coated SPIONs are 50 nm in diameter but that the magnetic cores are ∼ 10 nm. This suggests that although the hydrodynamic diameter is larger for the SPIONs compared to the SIPPs, the magnetic cores are similar in size and; therefore, the SIPP and SPION magnetic properties can be compared. Table II summarizes our characterizations of the μMAC particles using TEM, SQUID, and ICP-OES. It is clear that the volume magnetization of the SPIONs is ∼3.5-fold less than determined for our SIPPs. Next, we
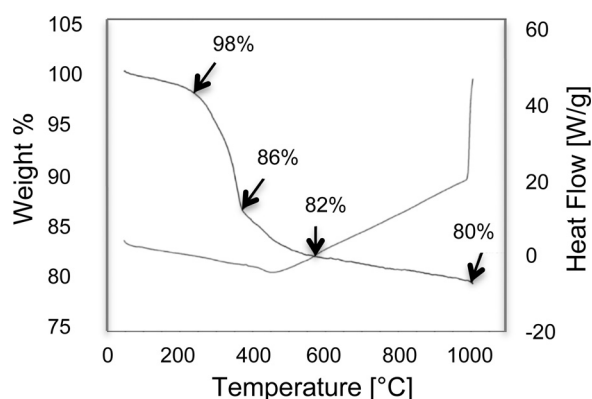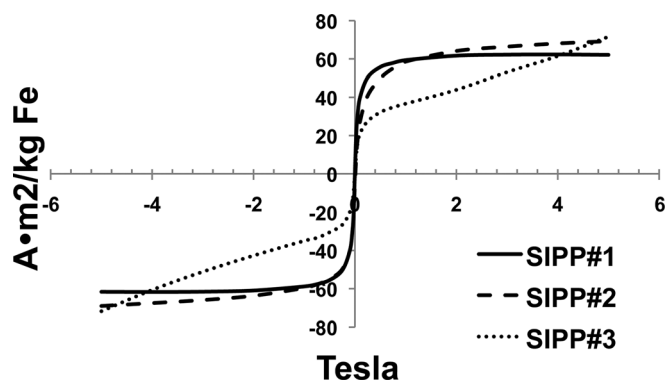
FIG. 2. Weight loss and heat flow curves for SIPP#1. Dried SIPPs were added to TGA sample cups and heated at 20 °C/h from room temperature to 1000 °C. The weight percent of organic coating and naked FePt was then extrapolated. The curve labeled with arrows shows the decrease in weight percent while the unlabeled curve shows the heat flow.

FIG. 3. Mass magnetization of SIPPs measured using SQUID and ICP-OES. 100 μL aliquots of SIPPs were evaporated in constricted NMR tubes and sealed. SQUID magnetometry data was collected at 310 K from −5 to 5 T. Also, 100 μL aliquots of SIPPs were added to conical tubes and analyzed with ICP-OES to determine the mass of iron in each SQUID sample. The solid line is for SIPP#1, the long dashed line is for SIPP#2, and the dotted line is for SIPP#3.
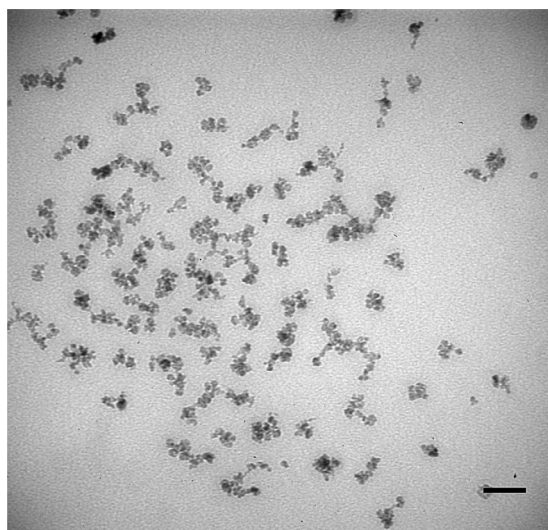
FIG. 4. Image of μMAC SPIONs acquired using transmission electron microscopy. A drop of μMAC SPIONS was applied to a carbon-coated grid. The sample was imaged at an acceleration voltage of 80 kV. Scale bar = 50 nm.
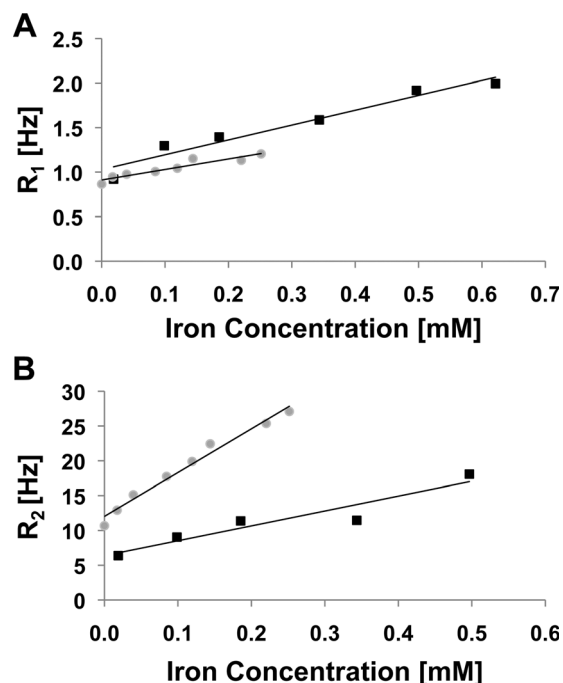

FIG. 5. Comparison of SIPP and SPION relaxivities measured at 4.7 T. Increasing concentrations of particles were added to 1% agarose and scanned at 4.7 T with TR = 10 s and TE = 40 ms. R_1 and R_2 values were calculated by taking the inverse of the T_1 and T_2 relaxation times. The relaxation rates (R_1 and R_2) were then plotted vs the iron concentration (mM Fe), measured using ICP-OES. The slope of the linear regression is the relaxivity of the specific particle at 4.7 T. Squares = SPIONs and circles = SIPPs. (A) Longitudinal relaxation rates. (B) Transverse relaxation rates.

prepared μMAC relaxivity samples by adding increasing amounts of SPIONS to 1% agarose.[9] We also prepared SIPP#2 relaxivity samples by first magnetically separating the SIPPs and then suspending the particles in the initial volume of a strong surfactant, RN-10, to disperse the hydrophobic SIPPs in the aqueous agarose. Increasing amounts of the RN-10 stabilized SIPPs were then added to 1% agarose in plastic sample tubes. Table III shows the relaxivities measured at 4.7 T, while Fig. 5 shows the longitudinal and transverse relaxation rates of the SIPPs and SPIONs as a function of iron concentration. It is apparent that the SIPPs have a threefold higher r_2 than the μMAC SPIONs and more than a fourfold increase in the r_2/r_1 ratio. The higher measured r_2/r_1 ratio would be favorable for a T_2-lowering MRI contrast agent. The SIPP#2 sample had a lower mass magnetization compared with the μMAC SPIONs, yet a much larger volume magnetization of approximately 7.4×10^5 A/m. This volume magnetization is in good agreement with previously reported volume magnetizations of SIPPs (between 6×10^5 A/m and 1×10^6 A/m).[10–12] Our result is novel, though, in that we have used safer methods, less reagents, and different temperatures to synthesize the particles for an MRI application. This difference in the volume magnetizations for the SPIONs and SIPPs may be due to the fact that

the SPIONs are encapsulated in dextran and the SIPPs are stabilized with the strong surfactant, RN-10. It is possible that the dextran coating decreases the relaxivities of the particles by preventing the necessary close approach of water molecules. A current focus in our lab is to encapsulate the SIPPs in phospholipids and again measure the relaxivities of these particles compared with SPIONS.[9] Overall, our data suggest that SIPPs can be tailored to optimize size and magnetic properties. In addition, SIPPs may be superior contrast agents in T_2-weighted imaging when compared to SPIONs.

IV. SUMMARY AND CONCLUSIONS

Synthesis of SIPPs, from low-toxicity precursors, was performed producing spherical particles in the range of 9.3–10 nm. The synthesized SIPPs showed increasing size and increasing iron to platinum stoichiometry when the molar concentration of iron precursor increased and when the amount of ODA was increased. The TGA results suggested that the particles were 80% naked FePt and 20% organic ligand, by mass. The saturation magnetization of the particles increased with increasing iron concentration, as measured with SQUID magnetometry. Further studies are needed to elucidate the mechanism of initial FePt nucleation and the crystalline and stability changes as the Fe to Pt stoichiometry is increased. The synthesized SIPPs showed increased r_2 and r_2/r_1 when compared with SPIONs, suggesting that SIPPs may be superior contrast agents for T_2-weighted MRI. Only limited cytotoxicity studies have been reported for SIPPs and have focused on

TABLE III. SIPP and SPION relaxivities measured at 4.7 T.

Variable	Unit	SPION[a]	SIPP#2
r_1	Hz/mM Fe	1.67[b]	1.18
r_2	Hz/mM Fe	21.37[b]	62.2
r_2^*	Hz/mM Fe	436[b]	253
r_2/r_1	—	13[b]	53

[a]MACS® iron oxide particles from Miltenyi Biotec.
[b]Taylor *et al*. (Ref. 9).

nonencapsulated SIPPs.[17] Silica encapsulated SIPPs have also been reported[18] but, to our knowledge, the cytotoxicity of encapsulated SIPPs has not been established. Determining the cytotoxicity of encapsulated SIPPs would be an important future endeavor.

[1] L. Han, U. Wiedwald, B. Kuerbanjiang, and P. Ziemann, Nanotechnology **20**, 285706 (2009).
[2] C. Antoniak *et al.*, Phys. Rev. Lett. **97**, 117201 (2006).
[3] S. Sun, C. B. Murray, D. Weller, L. Folks, and A. Moser, Science **287**, 1989 (2000).
[4] J. R. Kim, C. Rong, C. Liu, and P. Sun, Adv. Mater. **21**, 906 (2009).
[5] S. Sun, Adv. Mater. **18**, 403 (2006).
[6] L. C. Varanda and M. Jafelicci, Jr., J. Am. Chem. Soc. **128**, 11062 (2006).
[7] S. Maenosono, T. Suzuki, and S. Saita, J. Magn. Magn. Mater. **320**, 79 (2008).
[8] M. P. Morales *et al.*, J. Mater. Chem. **19**, 6381 (2009).
[9] R. M. Taylor, D. L. Huber, T. C. Monson, A. M. Ali, M. Bisoffi, and L. O. Sillerud, J. Nanopart. Res. **13**, 4717 (2011).
[10] F. Zhao, M. Rutherford, S. Y. Grisham, and X. Peng, J. Am. Chem. Soc. **131**, 5350 (2009).
[11] H. Zeng, J. Li, J. P. Liu, Z. L. Wang, and S. Sun, Nature **420**, 395 (2002).
[12] C. Xu, Z. Yuan, N. Kohler, J. Kim, M. A. Chung, and S. Sun, J. Am. Chem. Soc. **131**, 15346 (2009).
[13] K. Inomata, T. Sawa, and S. Hashimoto, J. Appl. Phys. **64**, 2537 (1988).
[14] W. S. Rasband, U.S. National Institutes of Health, Bethesda, MD, (1997–2009), http//rsb.info.nih.gov/ij/.
[15] Z. Shan, W. Yang, X. Zhang, Q. Huang, and H. Ye, J. Braz. Chem. Soc. **18**, 1329 (2007).
[16] V. Salgueirino-Maceira, L. M. Liz-Marzan, and M. Farle, Langmuir **20**, 6946 (2004).
[17] S. Maenosono, R. Yoshida, and S. Saita, J. Toxicol. Sci. **34**, 349 (2009).
[18] M. Aslam, L. Fu, S. Li, and V. P. Dravid, J. Colloid Interface Sci. **290**, 444 (2005).